Combustion and Flame 166 (2016) 98–112

Contents lists available at ScienceDirect

Combustion and Flame

journal homepage: www.elsevier.com/locate/combustflame

Fuel performances in Spark-Ignition (SI) engines: Impact of flame stretch

Pierre Brequigny[a,b,*], Fabien Halter[a], Christine Mounaïm-Rousselle[a], Thomas Dubois[b]

[a] Laboratoire PRISME, Université d'Orléans, INSA CVL, Orléans 45072, France
[b] Centre de Recherche de Solaize, TOTAL Marketing & Services, Solaize, France

ARTICLE INFO

Article history:
Received 11 June 2015
Revised 4 January 2016
Accepted 6 January 2016
Available online 8 February 2016

Keywords:
Flame stretch
Premixed combustion
Spark-Ignition engine

ABSTRACT

In a context of decreasing pollutant emissions, the transport sector has to tackle improvements to the engine concept as well as fuel diversification. The use of these different fuels often has an impact on the combustion performance itself. In the case of Spark Ignition (SI) engines, efficiency is a function of the combustion speed, i.e. the speed at which the fresh air–fuel mixture is consumed by the flame front. Every expanding flame is subject to flame curvature and strain rate, which both contribute to flame stretch. As each air–fuel mixture responds differently to flame stretch, this paper focuses on understanding the impact of flame stretch on fuel performances in SI engines. Different air–fuel mixtures (different fuels or equivalence ratios) with similar unstretched laminar burning speeds and thermodynamic properties but different responses to stretch were selected. The mixtures were studied in a turbulent spherical vessel and in an optical engine using Mie-Scattering tomography. The combustion phasing was also investigated in both optical and all-metal single cylinder engines. Results show that flame stretch sensitivity properties such as Markstein length and Lewis number, determined in laminar combustion conditions, are relevant parameters that need to be taken into consideration to predict the global performance of fuels, either experimentally or for modeling simulation.

1. Introduction

Nowadays, the automotive industry is facing a context of fuel diversification. Due to the increasingly restrictive standards on pollutants and CO_2 emissions, the car industry is developing new technologies that impact fuel development. Moreover to compensate for the depletion of fossil energy resources, oil companies have introduced Biofuels, used either pure or blended. The use of these fuels in a Spark-Ignition (SI) engine may induce a different combustion behavior and could therefore impact engine efficiency. To improve their products, oil companies seek to develop fuels that burn fast, evaporate easily, and have a high resistance to knock. For SI engines, the efficiency can be directly improved by increasing the area of the high-pressure loop on the *P*–*V* diagram and therefore by increasing the flame speed. The fundamental laminar burning speed S_L^0 is hence usually investigated as the first step in evaluating potential alternative fuels for SI engines [1–4]. Moreover it is a key parameter for combustion modeling in SI engines since the S_L^0 value is required in most existing models [5–10]. This burning speed corresponds to the speed of a one-dimensional planar adiabatic flame in laminar conditions without any instability and is a function of pressure, temperature, fuel and equivalence ratio. Nevertheless, S_L^0 cannot be considered as the speed of an expanding flame since expanding flames are subject to flame stretch, which is a compound of strain rate and flame curvature [11]. The flame stretch can be defined as the relative growth rate of the flame surface A [12]:

$$K = \frac{1}{A}\frac{dA}{dt} \tag{1}$$

Initially presented in the work of Karlovitz et al. [13] and Markstein [14], flame stretch is usually linearly linked [15] to the laminar flame speed S_b as below, with L_b the Markstein length and S_b^0 the unstretched laminar flame speed:

$$S_b = S_b^0 - L_b K \tag{2}$$

In some recent studies, a more realistic nonlinear relationship between flame speed and flame stretch has been used [16–18]:

$$\left(\frac{S_b}{S_b^0}\right)^2 \ln\left(\frac{S_b}{S_b^0}\right)^2 = -\frac{2L_bK}{S_b^0} \tag{3}$$

* Corresponding author at: Laboratoire PRISME, Université d'Orléans, INSA CVL, Orléans 45072, France.

E-mail addresses: pierre.brequigny@univ-orleans.fr (P. Brequigny), fabien.halter@univ-orleans.fr (F. Halter), christine.rousselle@univ-orleans.fr (C. Mounaïm-Rousselle), thomas.dubois@total.com (T. Dubois).

http://dx.doi.org/10.1016/j.combustflame.2016.01.005
0010-2180/

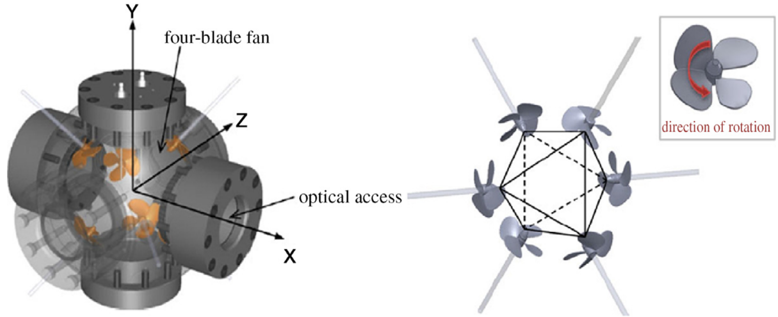

Fig. 1. Schematic view of the spherical vessel.

Under certain assumptions the unstretched laminar flame speed, S_b^0 is directly related to S_L^0 by using the expansion ratio ρ_b/ρ_u, where ρ_b and ρ_u are respectively the burnt and fresh gas densities:

$$S_L^0 = \frac{\rho_b}{\rho_u} S_b^0 \tag{4}$$

In Eqs. (2) and (3), the Markstein length L_b is a key parameter because it represents the flame stretch sensitivity of an air–fuel mixture. It is a function of the Zeldovich number, the flame thickness and particularly of the Lewis number *Le* (i.e. the ratio of the thermal diffusivity to the mass diffusivity). As the two parameters L_b and *Le* are strongly dependent on the fuel, the different responses of fuels to flame stretch will impact the flame propagation differently. While this effect has been fully investigated in laminar conditions [19–21] and even in turbulent conditions [22–24], only a few recent studies have addressed the effect of flame stretch in an SI engine [25–27]. Aleiferis et al. [25] compared methane, ethanol, butanol, iso-octane and gasoline flame propagation in an optical SI engine. Their results showed different flame radius evolutions and a ranking of the four mixtures in terms of Markstein lengths. The mixtures with the lowest Markstein lengths appeared to be those with the highest flame growth speed. However since the mixtures were studied at the same equivalence ratio, they present different unstretched laminar flame speeds. It could not be concluded from this study therefore whether the propagation differences were due to the flame stretch response rather than to a laminar flame speed ranking. Most CFD models require the unstretched laminar burning speed S_L^0 [5,7,8,28], often calculated by using correlations such as those of Metghalchi and Keck [29] or Gülder [30]. However, only a few models take into account the laminar flame speed dependence on the flame stretch with respect to the Markstein length or the Lewis number of the fuel–air mixture and use a stretched burning speed [6,7,9,10,31]. For instance, Dahms et al. [9,10] recently developed the SparkCIMM model. This model is based on the G-equation developments by Peters [7] in which the turbulent flame speed needs to be modeled. Dahms et al. proposed a model where the turbulent flame speed is computed from the stretched laminar burning speed calculated with a linear relation expressed by Eq. (2) and the model of Clavin [15].

To gain a better understanding of the impact of flame stretch on fuel combustion performance in SI engines and to assess how the different flame stretch responses of the mixtures can impact engine performance, an original experimental approach has been used here, covering numerous configurations from the simplest, a laminar spherical combustion vessel, to the most complicated, an all-metal single cylinder SI engine. The objectives of this study are then:

- to assess what is the consequence of the various flame stretch responses, i.e. the Markstein lengths of different mixtures on the flame propagation in a turbulent vessel at atmospheric pressure;
- to verify if the behaviors observed in the turbulent vessel are relevant to describe what happens in the engine by studying flame propagation in an optical engine;
- to see if some operating parameters of the engine such as the engine regime have an effect on the response to the flame stretch and if those effects can be linked to the observations made in the turbulent vessel;
- to assess the impact of the various flame stretch responses on the global combustion characteristics especially the combustion phasing which is directly linked to the engine yield;
- to check if the optical engine results can then be extrapolated to other kinds of engines by using an all-metal engine;
- and finally to determine whether flame stretch sensitivity should be considered as a key factor when developing and classifying a new fuel, and whether it should therefore be integrated in a CFD modeling approach.

2. Selection of different air–fuel mixtures

In order to focus on the impact of the different responses of the air/fuel mixtures to flame stretch, several mixtures were selected using the following criterion: mixtures with similar unstretched laminar flame speeds but different flame stretch sensitivities, i.e. different Markstein lengths and Lewis numbers. To measure these properties the classical method of spherical propagation was used. Three different fuels in lean conditions were used: iso-octane, close to gasoline, propane and methane. Lean mixtures of three different hydrocarbons were preferred in order to cover a large range of Lewis numbers [32,33] and because they are more suitable than rich ones for Spark-Ignition engine operations.

2.1. Experimental setup

To select the mixtures by measuring unstretched laminar flame speeds and Markstein lengths, a spherical vessel fully described by Galmiche et al. [34] was used (Fig. 1). The combustion chamber is a spherical stainless steel vessel with an inner diameter of 200 mm, equipped with four quartz windows with an inner diameter of 70 mm. Full details of the gas and liquid introduction and ignition procedure can be found in Galmiche et al. [35] and Broustail et al. [36,37]. 6 fans are used for the mixing process and the air/fuel mixture is ignited 5 s after stopping the fans to avoid any turbulence. Experiments were carried out at 1 bar and 400 K.

The flame speed and Markstein length were measured with Mie-Scattering tomography. The laser sheet was created in the *XOY* plane (Fig. 1) at the center of the chamber using a Nd:YAG Dual Hawk HP laser coupled with a spherical lens (focal length 300 mm) and a cylindrical lens (focal length 25 mm). The laser sheet was about 0.5 mm thick and laser pulses were synchronized with a